Density of single-particle states in a system of strongly correlated electrons in copper oxides

S. G. Ovchinnikov

L. V. Kirenskiĭ Institute of Physics Siberian Branch of the Russian Academy of Sciences, Krasnoyarsk
(Submitted 18 May 1993)
Zh. Eksp. Teor. Fiz. **104**, 3719–3734 (November 1993)

This paper suggests a method for calculating the single-particle Green function and the density of states in the multielectron theory within the framework of a generalized tight-binding approximation that allows for strong electron correlations. The densities of states for the CuO_2 plane undoped and lightly doped within holes are calculated, and states are shown to emerge with the insulator gap under doping.

1. INTRODUCTION

There is a large class of compounds in which electron correlations are strong and, hence, determine the basic physical properties. Among these are Mott-Hubbard insulators and insulators with a gap caused by charge-transfer processes.[1] Not only copper oxides belong to this class but so do other transition-metal oxides and many other compounds of transition and rare-earth elements.[2] Copper oxides have been chosen because studying their electronic structure in the insulator state and the variations of the structure caused by doping is important for understanding the mechanisms of high-T_c superconductivity.

Owing to the strong electron correlations, traditional methods of calculating the band structure such as the local density functional are inapplicable. For instance, for undoped insulators La_2CuO_4, Nd_2CuO_4, and $YBa_2Cu_3O_6$, the band theory gives a metallic state with a half-filled band (see Ref. 3 for a review). The band theory is equally inapplicable to lightly doped systems with a low concentration of carriers of the p- or n-type, for which there is experimental evidence of the existence of states in the gap of the deep-impurity-level type.[4]

At present there are no band-structure calculations that start from first principles and allow correctly for strong electron correlations. A generalized tight-binding method has been suggested to allow for strong correlations in a semiphenomenological setting.[5] In this method strong correlations are taken into account exactly, and the multiband model in the Hubbard-operator representation is reduced to a generalized Hubbard model with a large number of multielectron states per site.

A dispersion equation for the spectrum of single-particle Fermi excitations (holes for the CuO_2 plane) was obtained in the generalized tight-binding method in Ref. 6. This equation was later used[7] to calculate the band structure of undoped La_2CuO_4 and Nd_2CuO_4.

The cited papers[5–7] do not consider the density of states, since its calculation with allowance for strong correlations is much more complicated than finding the dispersion law. The physical reason for these difficulties lies in the fact that the statistics of single-particle states in strongly correlated systems depends on the occupation numbers. For instance, in the undoped cases, even allowing for twofold degeneracy in spin, each Hubbard band contains only one electron rather than two as in the case of free electrons. Doping only complicates matters because the number of states in each band becomes a function of the electron concentration. All this leads to a situation in which simple integration over constant-energy surfaces, as is done in single-electron band theory, does not permit finding the density of states. Mathematically the problem is that calculating the spectrum requires knowing only the dispersion equation, that is, only the denominator of the Green function, while calculating the density of states requires knowing the entire Green function. Since the Green functions in the multilevel Hubbard model are high-dimension matrices (e.g., for the CuO model[5] with six orbitals per unit cell in the limit of $U_d = \infty$ and $U_p = \infty$ in the undoped case, one is forced to deal with a 44-by-44 matrix, and in the doped case the dimension of the matrix increases sharply), calculating the imaginary part of the Green function and its integral over the Brillouin band requires a much greater volume of calculations than simply solving the dispersion equation.

In this paper the Green function is found explicitly by a method that does not involve calculating high-dimension inverse matrices. Moreover, in this approach the dimension of the system of linear equations whose solutions determine the Green function does not depend on the electron density; it is rather given by the number of orbitals in a cell, as in ordinary band theory. The solution method is based on employing the multiplicative nature of the intercell interaction potential. Such an approach was used earlier in the theory of anisotropic Heisenberg magnetic substances.

2. THE MULTIELECTRON MODEL OF COPPER OXIDES

Photoelectron data suggests that the conduction-band bottom and the valence band at a depth of 6–7 eV are formed by the p-orbitals of oxygen and d-orbitals of copper, with the other filled states lying lower and the vacant states higher. For this reason we limit our discussion to the calculation of hybridized p-d-states of the CuO_2 plane, assuming that for vacant and filled bands the strong-correlation effects are insignificant, that is, the bands can

 1063-7761/93/110781-10$10.00

be taken from standard band calculations and simply superimposed on the p-d-bands of strongly correlated electrons.

We write the Hamiltonian of p- and d-electrons of the CuO_2 plane in the hole representation as follows:

$$
\begin{aligned}
&H=H_d+H_p+H_{pd}+H_{pp},\\
&H_d=\sum_r H_d(r),\\
&H_d(r)=\sum_{\lambda\sigma}\left[(\varepsilon_{d\lambda}-\mu)d^\dagger_{r\lambda\sigma}d_{r\lambda\sigma}+\frac{1}{2}U_d n^\sigma_{r\lambda}n^{-\sigma}_{r\lambda}\right]\\
&\qquad+\sum_{\sigma\sigma'}(V_d n^\sigma_{r1}n^{\sigma'}_{r2}-J_d d^\dagger_{r1\sigma}d_{r1\sigma'}d^\dagger_{r2\sigma'}d_{r2\sigma}),\\
&H_p=\sum_r H_p(i),\\
&H_p(i)=\sum_{\alpha\sigma}\left[(\varepsilon_{p\alpha}-\mu)p^\dagger_{i\alpha\sigma}p_{i\alpha\sigma}+\frac{1}{2}U_p n^\sigma_{i\alpha}n^{-\sigma}_{i\alpha}\right]\\
&\qquad+\sum_{\sigma\sigma'}(V_p n^\sigma_{i1}n^{\sigma'}_{i2}-J_p p^\dagger_{i1\sigma}p_{i1\sigma'}p^\dagger_{i2\sigma'}p_{i2\sigma}),\\
&H_{pd}=\sum_{\langle i,r\rangle}H_{pd}(i,r),\\
&H_{pd}(i,r)=\sum_{\alpha\lambda\sigma\sigma'}(T_{\lambda\alpha}p^\dagger_{i\alpha\sigma}d_{r\lambda\sigma}+\text{H.c.}+V_{\lambda\sigma}n^\sigma_{r\lambda}n^{\sigma'}_{i\alpha}\\
&\qquad-J_{\alpha\lambda}d^\dagger_{r\lambda\sigma}d_{r\lambda\sigma'}p^\dagger_{i\lambda\sigma'}p_{i\alpha\sigma}),\\
&H_{pp}=\sum_{\langle i,j\rangle}\sum_{\alpha\beta\sigma}(t_{\alpha\beta}p^\dagger_{i\alpha\sigma}p_{j\beta\sigma}+\text{H.c.}),
\end{aligned}
\tag{1}
$$

where ε_p and ε_d are the single-particle energies of p- and d-holes, $U_p(U_d)$ and $V_p(V_d)$ the matrix elements of the interatomic Coulomb repulsion on the same and on different orbitals of oxygen (copper), $J_p(J_d)$ the Hund exchange integrals, $T_{\lambda\sigma}$ and $t_{\alpha\beta}$ the matrix elements of p-d- and p-p-hopping between nearest neighbors, and $V_{\lambda\alpha}$ and $J_{\lambda\alpha}$ the matrix elements of the Coulomb and exchange interaction between the copper-oxygen nearest neighbors. The first two terms in Eq. (1) describe interatomic p-d-hopping and interactions and p-p-hopping. The important orbitals are $d_{x^2-y^2}$ ($\lambda=1$) and d_{z^2} ($\lambda=2$) for copper and p_x ($\alpha=1$) and p_y ($\alpha=2$) for oxygen. We introduce the notation

$$
T_{x^2-y^2,p_x}=T_{pd},\quad V_{x^2-y^2,p_x}=V_{pd},
$$

$$
J_{x^2-y^2,p_x}=J_{pd},\quad t_{x,y}=t_{pp}.
$$

3. THE TIGHT-BINDING METHOD WITH ELECTRON CORRELATIONS

As is known, correlations are well accounted for in the atomic limit of models of the Hubbard type, and interatomic hopping in the band limit. A cluster method of calculation was developed in Refs. 5 and 6 to account for correlations and covalent effects in a meaningful manner.

In the generalized tight-binding method, band-structure calculations are done in two stages. In the first the lattice is divided into nonoverlapping clusters (elementary cells) within each of which the eigenvalue problem for Hamiltonian (1) is solved exactly and Hubbard operators are constructed in whose representation the cell Hamiltonian is diagonal. In the second stage, intercell hopping and interactions are reduced exactly to hopping between the sites of the multilevel Hubbard model. The resulting model can then be studied by various methods known to be valid for the ordinary Hubbard model.

For laminar copper oxides the simplest cell consists of a CuO_2 cluster O–Cu–O. In the hole representation the vacuum state $|0\rangle$ with $n=0$ holes corresponds to the $p^6d^{10}p^6$ configuration. In the stoichiometric compounds La_2CuO_4 and Nd_2CuO_4 there are $n=1$ holes assigned to each cluster, and the eigenstates are various mixtures of $p^5d^{10}p^6$ and $p^6d^9p^6$ configurations. In hole doping there appear clusters with $n=2$ holes in which $p^6d^8p^6$, $p^5d^9p^6$, $p^5d^{10}p^5$, and $p^4d^{10}p^6$ configurations are mixed. Let $|n,l\rangle$ be the set of eigenstates of Hamiltonian (1) with energies $E(n,l)$ for a cluster with n holes, with the index l designating all other quantum numbers, including orbital and spin quantum numbers. Knowing the complete set of states of a cluster makes it possible to construct the Hubbard operators $X^{pg}\equiv|p\rangle\langle g|$ in whose representation the intracell part of Hamiltonian (1) has the form (for the cell with number f)

$$
H_0=\sum\sum(E(n,l)-n\mu)X_f^{nl,nl}. \tag{2}
$$

The creation of a single-particle Fermi excitation (hole) is related in the multielectron approach to the transition of the system from the n-particle state to the $(n+1)$-particle state. In building a consistent theory of perturbations in intercell hopping it has been found convenient (see Ref. 9) to assign to each pair consisting of an initial and final state a root vector, namely,

$$
(n,l_1;n+1,l_2)\to\alpha_m,
$$

where the subscript m numbers the various Fermi excitations. We denote the Hubbard operator in compact form as follows:

$$
X_f^{n,l_1;n+1,l_2}\to X_f^{\alpha_m}\to X_f^m.
$$

In the Hubbard-operator representation the operators representing the annihilation and creation of a hole in cell f on orbital λ and with spin projection σ are then

$$
a_{f\lambda\sigma}=\sum_m\gamma_{\lambda\sigma}(m)X_f^m,\quad a^\dagger_{f\lambda\sigma}=\sum_m\gamma^\dagger_{\lambda\sigma}(m)X_f^{\dagger m}, \tag{3}
$$

with the matrix elements

$$
\gamma_{\lambda\sigma}(m)\langle n,l_1|a_{f\lambda\sigma}|n+1,l_2\rangle.
$$

For a CuO_2 cell there are six different orbital states in the Hamiltonian model (1):

$$
\{\lambda\}=\{p_x(1),p_y(1),d_{x^2-y^2},d_{z^2},p_x(2),p_y(2)\}.
$$

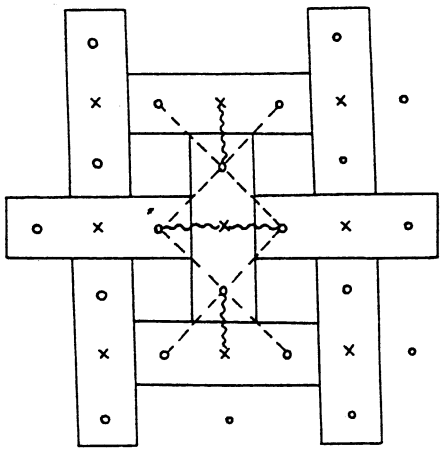

FIG. 1. Double-sublattice partitioning of the CuO_2 plane: ×—copper; ○—oxygen. The wavy and dashed lines correspond to intercluster copper-oxygen and oxygen-oxygen hopping.

In the intracell Hubbard-operator representation the intercell-hopping Hamiltonian has the form[6]

$$H_1=\sum_{mn}\sum_{k}[(A^{mn}_{FG}(k)+B^{mn}_{FG}(k))X^m_k Y^n_k+\text{H.c.}], \quad (4)$$

where the A and B matrices correspond to p-d and p-p hopping (below these are given explicitly). Here we have gone over to a double-sublattice elementary cell consisting of two CuO_2 clusters (Fig. 1), and X_k and Y_k are the Fourier transforms of the Hubbard operators in the sublattices F and G. We introduce the double-lattice Green function

$$\hat{D}_{mn}(k,E)=\begin{pmatrix} \langle\langle X^m_k | X^{\dagger n}_k\rangle\rangle, & \langle\langle X^m_k | Y^{\dagger n}_k\rangle\rangle \\ \langle\langle Y_k | X_k\rangle\rangle, & \langle\langle Y_k | Y_k\rangle\rangle \end{pmatrix}. \quad (5)$$

The zeroth-order Green function for Hamiltonian (2) can be calculated exactly:

$$D^{ij}_{(0),mn}(k,E)=\delta_{ij}\delta_{mn}\frac{F_m}{E-\Omega_m}, \quad (6)$$

where the intracluster excitation energy

$$\Omega_m\equiv\Omega(\alpha_m)=E(n+1,l_2)-E(n,l_1), \quad (7)$$

and the end factor F_m differs from unity because of the complicated commutation relations existing for the Hubbard operators,

$$F_m=\langle\{X^m,X^{\dagger m}\}_+\rangle=\langle X^{n,l_1;n,l_1}\rangle+\langle X^{n+1,l_2;n+1,l_2}\rangle. \quad (8)$$

In the diagrammatic technique for the Hubbard operators,[9] the Hartree–Fock approximation is simply the well-known Hubbard-I approximation. In this approximation the Green function (5) can be found by solving the equation

$$\hat{D}^{-1}=\hat{D}_0^{-1}-\hat{A}-\hat{B}, \quad (9)$$

whose determinant yields the hole spectrum. The occupation numbers, which determine the end factors, are expressed in a standard manner in terms of the imaginary parts of the diagonal elements of the Green function (5) and can be found together with the chemical potential by solving the self-consistency equation

$$\sum_{nl} n\langle X^{n,l;n,l}_f\rangle=n_h,$$

where n_h is the hole concentration per cluster. In our case $n_h=1+x$. Since $1<n_h<2$, only single-particle and two-particle states $|n,l\rangle$ contribute to the equation for the chemical potential. In contrast to the Hubbard model with four states at a site ($|0\rangle$, $|+1/2\rangle$, $|-1/2\rangle$, and $|2\rangle$), in our theory the number of states in a cell is large. For instance, in model (1) with six atomic orbitals there is one vacuum state $|0\rangle$ and twelve single-hole states (with allowance for spin). For $n=2$; even in the simplest limit of $U_d=\infty$ and $U_p=\infty$, the number of states is $2^2\times\binom{6}{2}=60$. The dimension of matrix (5) is determined by the number of nonzero matrix elements $\gamma(\alpha_m)$ and end factors F_m. In the undoped case for the CuO_2 model with $n=1$ the dimension is 44 by 44, while in the doped case new allowed transitions emerge and the D-matrix is 56 by 56. Since to calculate the density of states an integral is evaluated in the k-space, finding the Green function at each point of the k-space requires a large volume of calculations. In Sec. 4 we will find for Eq. (9) an explicit solution which greatly simplifies the calculation of the density of states.

4. CALCULATING THE GREEN FUNCTIONS

At $T=0$ only the occupation numbers of the ground states are nonzero. At $n=1$ the wave function of the ground level is ($\sigma=+,-$)

$$|1,\sigma\rangle=u|0;x^2-y^2,\sigma;0\rangle-v(|x,\sigma;0;0\rangle+|0;0;x,\sigma\rangle)\frac{1}{\sqrt{2}},$$

$$u^2=\left(1+\frac{\delta}{\nu}\right)\frac{1}{2},\quad v^2=1-u^2,\quad \delta=\varepsilon_p-\varepsilon_d,\quad \nu^2=\delta^2+8T^2_{pd}.$$

The energy of state $|1,\sigma\rangle$ is $E_{1\sigma}=\varepsilon_d+1/2(\delta-\nu)$. The two-particle states of a cluster were found in Ref. 5 with exact allowance for all Coulomb matrix elements and p-d-hybridization in the limit of $U_d=\infty$ and $U_p=\infty$, while exchange interactions were taken into account in first-order perturbation theory. The intratomic matrix elements J_p and J_d are positive (according to Hund's rule). For interatomic exchange both variants, $J_{pd}>0$ and $J_{pd}<0$, are possible. The two-particle ground state $|2,0,S,M\rangle$ may be a spin singlet $S=0$, $M=0$ or triplet $S=1$, $M=+1,-1,0$. The wave functions of the singlet and triplet are

$$|2,0,S,M\rangle = u_0(|x,+;0;x,-\rangle \mp |x,-;0;x,+\rangle)\frac{1}{\sqrt{2}}$$
$$-v_0(|0;x^2-y^2,+;x,-\rangle$$
$$\mp|0;x^2-y^2,-;x,+\rangle+|x;-;x^2-y^2,+;0\rangle$$
$$-|x,+;x^2-y^2,-;0\rangle)\tfrac{1}{2}.$$

The energies E_0 and E_1 of, respectively, the singlet and triplet are

$$E_0,1 = 2\varepsilon_d+\frac{1}{2}(3\delta+V_{pd}-\nu_0)\pm v_0^2 J_{pd}.$$

The parameter J_{pd} is the effective exchange parameter, determined by both the direct exchange matrix element and indirect antiferromagnetic exchange of the Zhang–Rice type.[11] Allowing for an additional weak p-p-hopping leads to the appearance of new contributions to the effective exchange depending on the sign of t_{pp} (see Refs. 12 and 13). Exact analysis of the conditions for the two-particle ground state to be a spin singlet or for it to be a triplet requires determining a certain region in the multidimensional space of parameters of the Hamiltonian. Solving such a problem lies outside the scope of the present paper. We allow for both states, and if variation of parameters leads to crossover between the states, the occupation numbers vary self-consistently, too. This leads to a difference between the density of states for the singlet and the triplet, which is discussed below.

The excited states for $n=0,1,2$ can be written in a similar manner. For one thing, two-particle excited states contain contributions from the configurations of neutral oxygen and trivalent copper. These states are not written here; the interested reader can find them in Ref. 5. Knowing the explicit form of the wave functions with $n=0,1,2$ makes it possible to calculate the fractional parentage coefficients in (3). It can easily be shown that the intercell-hopping Hamiltonians $T_{pd}p_i^\dagger d_j$ and $t_{pp}p_i^\dagger p_j$ have the form (4), and the p-d-hopping matrix A and the p-p-hopping matrix B can be written as sums of split matrices:

$$A_{FG}^{mn}(k) = A_1(k)\gamma_2(m)\gamma_1(n)+A_2(k)\gamma_3(m)\gamma_1(n)$$
$$+A_3(k)\gamma_1(m)\gamma_2(n)+A_4(k)\gamma_1(m)\gamma_3(n), \quad (10)$$

$$B_{FG}^{mn}(k) = B_1(k)\gamma_2(m)\gamma_2(n)+B_2(k)\gamma_2(m)\gamma_3(n)$$
$$+B_3(k)\gamma_3(m)\gamma_2(n)+B_4(k)\gamma_4(m)\gamma_4(n)$$
$$+B_5(k)\gamma_4(m)\gamma_5(n)+B_6(k)\gamma_5(m)\gamma_5(n)$$
$$+B_7(k)\gamma_5(m)\gamma_4(n),$$

where the matrix elements $\gamma_\lambda(m)$ are listed in Table I, in which

$$\gamma_0 = uv_0+u_0v, \quad \gamma_1 = uu_0-vv_0,$$
$$\gamma_2 = uu_1+vv_1, \quad \gamma_3 = uv_1-u_1v,$$
$$\gamma_4 = uu_2+vv_2, \quad \gamma_5 = uv_2-u_2v,$$

the coefficients u_i and v_i $(i=0,1,2)$ obey the relationships

$$u_i^2 = \frac{1}{2}\left(1-\frac{\Delta_i}{\nu_i}\right), \quad v_i^2 = 1-u_i^2, \quad \nu_i^2 = \Delta_i^2+8T_{pd}^2, \quad \delta = \varepsilon_p-\varepsilon_d,$$

$$\Delta_0 = \delta-v_{pd}, \quad \Delta_1 = v_{pd}-\delta-\tfrac{1}{2}v_p, \quad \Delta_2 = v_d-v_{pd}-\delta,$$

and $\sigma = \pm 1/2$ corresponds to the two spin projections. The band index λ in $\gamma_\lambda(m)$ stands for the following orbitals:

$$\lambda = 1-d_{x^2-y^2}, \quad \lambda = 2-[p_x(1)+p_x(2)]\frac{1}{\sqrt{2}},$$

$$\lambda = 3-[p_x(1)-p_x(2)]\frac{1}{\sqrt{2}},$$

$$\lambda = 4-p_y(1), \quad \lambda = 5-p_y(2), \quad \lambda = 6-d_{z^2}.$$

The number m of Fermi states listed in Table I corresponds to all possible hole states with nonzero matrix elements at $T=0$. For $T\neq 0$, generally speaking, the occupation numbers of the excited states with $n=1$ and $n=2$ are nonzero, which means taking into account the contributions of all states. But if we ignore the exponentially small contributions $\sim\exp(-\Delta E/T)$, where ΔE is the level separation, only the states listed in Table I will be left.

Here $m=1$ corresponds to creation of a hole in the vacuum state accompanied by the $|0\rangle \to |1,\sigma\rangle$ transition, while the other values $m>1$ correspond to creation of a hole accompanied by a transition to the two-particle state, $|1,l_1,\sigma\rangle \to |2,l_2,\sigma\rangle$. The energy of all excitations, Ω_0 can be found from a cluster calculation.

The functions A_i and B_i in (10) are

$$A_1 = 2T_{pd}\cos k_x a, \quad A_2 = -i2T_{pd}\sin k_x a,$$

$$A_3 = 2T_{pd}\cos k_y a, \quad A_4 = -i2T_{pd}\sin k_y a,$$

$$B_1 = 4t_{pp}(\cos k_x a+\cos k_y a), \quad B_2 = -i4t_{pp}\sin k_y a, \quad (11)$$

$$B_3 = -i4t_{pp}\sin k_x a, \quad B_4 = B_6^*, \quad B_5 = B_7^*,$$

$$B_6 = t_{pp}(\exp ik_x a+\exp ik_y a),$$

$$B_7 = t_{pp}[\exp ik_x a+\exp(-ik_y a)].$$

To calculate the Green functions, we employ a method suggested in Ref. 8 for solving problems with a split intercell-interaction matrix. In the case at hand we must deal with sums of split matrices (10), which requires a simple generalization of the method of Ref. 8.

We introduce the auxiliary Green functions

$$\hat{D}_{\lambda,n} = \sum_m \gamma_\lambda(m)\hat{D}_{n,m},$$

$$\hat{F}_{\lambda_1\lambda_2} = \sum_m \gamma_{\lambda_1}(m)\gamma_{\lambda_2}(m)\hat{D}_{(0),n},$$

using which we can write the system of equations for the Green functions (5) in the approximation of the

TABLE I. The matrix elements needed for representing the Fermi operators in terms of Hubbard operators; $\sigma = \pm 1/2$.

m	$\gamma_{x^2-y^2}$	γ_+	γ_-	γ_{1y}	γ_{2y}	γ_{z^2}	m	$\gamma_{x^2-y^2}$	γ_+	γ_-	γ_{1y}	γ_{2y}	γ_{z^2}
1	u	$-v/\sqrt{2}$	0	0	0	0	18	0	0	0	$-\gamma_3/\sqrt{2}$	0	0
2	$\sigma v v_0\sqrt{2}$	$-\sigma\gamma_0$	0	0	0	0	19	0	0	0	$-\gamma_3$	0	0
3	0	0	$-\gamma_0/2$	0	0	0	20	0	0	0	0	$\sigma\gamma_3/\sqrt{2}$	0
4	0	0	0	0	0	0	21	0	0	0	0	$-\gamma_3/\sqrt{2}$	0
5	0	0	0	$\sigma\gamma_2\sqrt{2}$	0	0	22	0	0	0	0	$-\gamma_3$	0
6	0	0	0	$-\gamma_2/\sqrt{2}$	0	0	23	v_0	$-u_0/\sqrt{2}$	0	0	0	0
7	0	0	0	$-\gamma_2$	0	0	24	$u_0/2$	$-u_0/2$	0	0	0	0
8	0	0	0	0	$\sigma\gamma_2\sqrt{2}$	0	25	0	0	$-\sigma u_0$	0	0	0
9	0	0	0	0	$-\gamma_2/\sqrt{2}$	0	26	0	0	$\gamma_1/\sqrt{2}$	0	0	0
10	0	0	0	0	$-\gamma_2$	0	27	0	0	$\gamma_1/2$	0	0	0
11	0	0	$-\sigma u$	0	0	0	28	0	$\sigma\gamma_1$	0	0	0	0
12	$-v/\sqrt{2}$	0	$-u/2$	0	0	0	29	0	0	0	0	0	γ_4
13	$-v$	$-u/\sqrt{2}$	0	0	0	0	30	0	0	0	0	0	$\gamma_4/\sqrt{2}$
14	$\frac{-\sigma v u}{\sqrt{2}}$	$\sigma\gamma$ 0	0	0	0	0	31	0	0	0	0	0	$\sigma\gamma_4/\sqrt{2}$
15	0	0	$\gamma_1/2$	0	0	0	32	0	0	0	0	0	γ_5
16	0	0	$\gamma_1/\sqrt{2}$	0	0	0	33	0	0	0	0	0	$\gamma_5/\sqrt{2}$
17	0	0	0	$\sigma\gamma_3/\sqrt{2}$	0	0	34	0	0	0	0	0	$\sigma\gamma_5\sqrt{2}$

Hubbard-I type (or in the Hartree–Fock approximation using the diagrammatic technique of Ref. 9) in the following manner:

$$\begin{aligned} D^{11}_{mn} = D^{11}_{(0),m}\delta_{mn} + D^{11}_{(0),m}\{&[A_1\gamma_2(m) + A_2\gamma_3(m)]D^{21}_{1,n} \\ &+ [A_3\gamma_1(m) + B_1\gamma_2(m) + B_3\gamma_3(m)]D^{21}_{2,n} \\ &+ [A_4\gamma_1(m) + B_2\gamma_2(m)]D^{21}_{3,n} \\ &+ [B_4\gamma_4(m) + B_7\gamma_5(m)]D^{21}_{4,n} \\ &+ [B_5\gamma_4(m) + B_6\gamma_5(m)]D^{21}_{5,n}\}, \end{aligned} \tag{12}$$

$$\begin{aligned} D^{21}_{mn} = D^{22}_{(0),m}\{&[A^*_3\gamma_2(m) + A^*_4\gamma_3(m)]D^{11}_{1,n} \\ &+ [A^*_1\gamma_1(m) + B^*_1\gamma_2(m) + B^*_2\gamma_3(m)]D^{11}_{2,n} \\ &+ [A^*_2\gamma_1(m) + B^*_3\gamma_2(m)]D^{11}_{3,n} \\ &+ [B^*_4\gamma_4(m) + B^*_5\gamma_5(m)]D^{11}_{4,n} \\ &+ [B^*_6\gamma_5(m) + B^*_7\gamma_4(m)]D^{11}_{5,n}\}. \end{aligned}$$

Multiplying Eqs. (12) term by term into $\gamma_\lambda(m)$ and summing over m, we arrive at the following system of linear equations for the functions $D^{11}_{\lambda,n}$ and $D^{21}_{\lambda,n}$:

$$(\hat{M} - \hat{I})\mathbf{D} = \mathbf{D}_0, \tag{13}$$

where $\mathbf{D}$ is the column vector corresponding to the row

$$\mathbf{D}^\dagger = (D^{11}_{1,n}, D^{21}_{1,n}, D^{11}_{2,n}, D^{21}_{2,n}, D^{11}_{3,n}, D^{21}_{3,n}, D^{11}_{4,n}, D^{21}_{4,n}, D^{11}_{5,n}, D^{21}_{5,n}),$$

and the matrix M can be expressed in terms of the function $F_{\lambda_1\lambda_2}$ (its explicit form is given in the Appendix). What is important is that the dimension of matrix M is determined by the number of atomic orbitals considered rather than by the number of various cluster states. The first number is much smaller than the second and independent of the choice of cluster.

Thus, instead of calculating the inverse matrix (9), we have reduced the problem to solving the matrix equation (13), whose dimension is much lower. Substituting the solution to (13) into (12), we find the Green functions (5). It can easily be verified that the dispersion law for quasiparticles is the same whether we determine it from the determinant of (13) or of (9). The additional factors

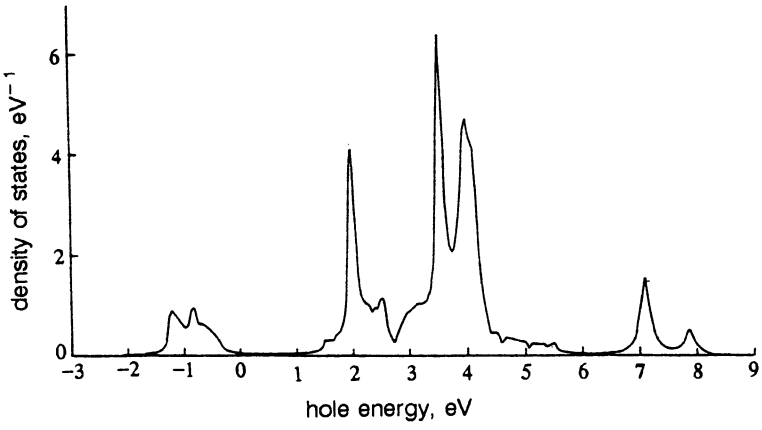

FIG. 2. Density of hole states of an undoped CuO_2 plane.

$\Omega(m)$ in (13) corresponding to local cluster modes are unimportant since they contribute nothing to the density of states.

5. THE DENSITY OF HOLE STATES

In terms of the initial atomic orbitals, the partial density of states is

$$N_\lambda(E)=-\frac{1}{\pi}\,\mathrm{Tr}\;\mathrm{Im}\langle\langle a_{i\lambda\sigma}|a^\dagger_{i\lambda\sigma}\rangle\rangle_{E+i\varepsilon}.$$

Since representation (3) is exact, it yields the sum rule

$$\langle\{c_{i\lambda\sigma},c^\dagger_{i\lambda\sigma}\}_+\rangle=\sum_m|\gamma_\lambda(m)|^2F_i(m)=1, \tag{14}$$

which ensures conservation of the total number of states when calculating the density of states in the Hubbard-operator representation:

$$N_\lambda(E)=-\frac{1}{\pi}\sum_m|\gamma_\lambda(m)|^2\,\mathrm{Tr}\;\mathrm{Im}\;\hat{D}(E+i\varepsilon). \tag{15}$$

This is directly verifiable if we substitute the zeroth-order Green function (6) into (15):

$$\int N^{(0)}_\lambda(E)dE=\frac{2}{N}\int\sum_{k\sigma}\sum_m|\gamma_\lambda(m)|^2F(m)\delta(E-\Omega_m)dE$$

$$=\frac{2}{N}\sum_{k\sigma}1=2. \tag{16}$$

The final expression for the total density of hole states is

$$N(E)=-\frac{2}{N}\sum_{k\sigma}\sum_{\lambda m}|\gamma_\lambda(m)|^2\frac{1}{\pi}\,\mathrm{Im}[D^{11}_{mm}(k,E+i\varepsilon)$$

$$+D^{22}_{mm}(k,E+i\varepsilon)]. \tag{17}$$

A package of programs named QPDOS was implemented to calculate the density of states following the algorithm for Green-function calculations described above. The sum over the quasimomemtum was calculated by integrating over the Brillouin zone, and all delta functions in

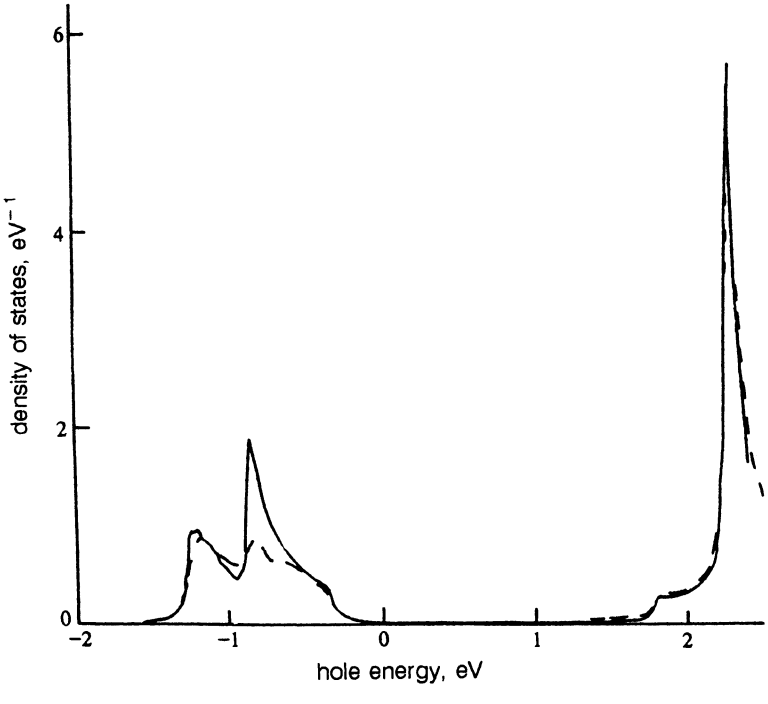

FIG. 3. Variation of the density of states caused by an increase in resolution. The dashed curve corresponds to $\varepsilon=0.1$ and the solid curve to $\varepsilon=0.05$.

(17) were replaced by Lorentzian curves with a half-width ε. The majority of calculations were performed with $\varepsilon=0.1$ eV, which corresponds to the highest-possible resolution of such methods as photoelectron spectroscopy.

Figure 2 depicts the density of hole states for the undoped CuO_2 plane, and the model parameters correspond[7] to undoped La_2CuO_4 (in electron volts):

$$U_d=\infty,\quad U_p=\infty,\quad V_d=4.5,\quad V_p=3,\quad V_{pd}=0.6,$$
$$j_p=j_d=0.5,\quad j_{pd}=0.2,\quad T_{pd}=1,\quad t_{pp}=0.2, \qquad (18)$$
$$\delta=2,\quad \Delta_d=\varepsilon_{d_{z^2}}-\varepsilon_{d_{x^2-y^2}}=1.5,\quad \Delta_p=\varepsilon_{p_x}-\varepsilon_{p_y}=0.8.$$

A detailed discussion of these parameters and their comparison with the data of other researchers can be found in Ref. 10. The hole energy is measured from the atomic level of the $d_{x^2-y^2}$ orbital, $\varepsilon_d=0$.

The lower Hubbard band in Fig. 2 (this is the conduction band in the electron representation) obeys the dispersion law

$$E_1(\mathbf{k})=\Omega_1\pm T_1F(1)\gamma(\mathbf{k}),$$

where

$$T_1=T_{pd}\frac{uv}{\sqrt{2}},\quad \gamma(\mathbf{k})=2(\cos k_xa+\cos k_ya).$$

The emergence of two branches is due to the double-sublattice structure. The bandwidth $\sim T_1$ is much smaller than T_{pd} because of correlation band narrowing.

The upper Hubbard band is separated from the lower one by a gap, which in our case is infinite. Inside this gap lies the hybridized p-d-band consisting of a large number of narrow subbands and obeying a complex dispersion law. The width of the lower of these subbands is of the order of $T_2=T_{pd}vv_0(uv_0+u_0v)/2\sqrt{2}$.

The insulator gap has a complex nature: it is formed both by charge-transfer processes and by Coulomb and exchange interactions. In conditions when the Hubbard-I approximation is valid, the bond-to-band transition probability is low and we have the following expression for the gap:

$$E_g=E_g^0-2T_1-2T_2, \qquad (19)$$

where E_g^0 is determined by intracluster energies:

$$E_g^0=\sqrt{\delta^2+8T_{pd}^2}-\frac{1}{2}\sqrt{(\delta-V_{pd})^2+8T_{pd}^2}$$
$$+\frac{1}{2}(\delta+V_{pd})-v_0^2|J_{pd}|.$$

We see that in the limit of $\delta\gg T_{pd},V_{pd}$, the main contribution to the gap is provided by the charge-transfer energy, $E_g^0\sim\delta$.

The condition for the collapse of the gap is $T_1+T_2\sim E_g^0$, in which case the Hubbard-I approximation becomes invalid. In the language of diagrams as applied to Hubbard operators this means that we must allow for single-loop contributions to the mass operator.[9] When the parameters are those specified in (18), which we assume typical for all undoped and lightly doped copper oxides, both T_1 and T_2 are much smaller than E_g^0, and the criterion of applicability of the Hubbard-I holds true.

Let us now study the filling of the bands. The lower Hubbard band in the undoped case $n=1$ is completely filled. Formally the reason for this is that the factor $F(m)=1/2$ for $m=1$, and it is these states that form the band. Physically the explanation lies in the strong correlations that change the statistics, an aspect discussed in Sec. 1. Thus, the Fermi level lies in a gap $E_g=2$ eV, and the hole states above the gap (the valence band in the electron representation) are unfilled. The total width of the p-d-hybridized valence band is close to 6 eV.

Since the atomic-orbital base is limited, it is useless to calculate the states far from the gap. For instance, accord-

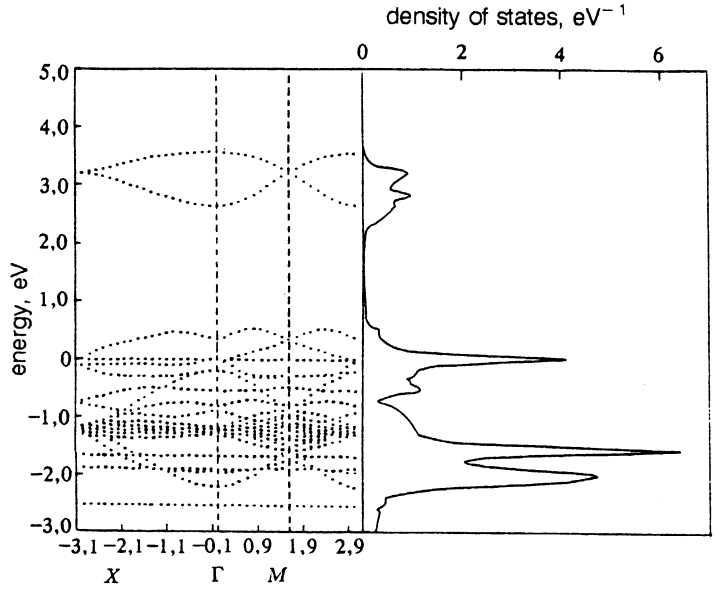

FIG. 4. Comparison of the band structure and density of . quasiparticle states in the electron representation. Energies are measured from the level $\Omega(m=2)$, which forms the top of the valence band.

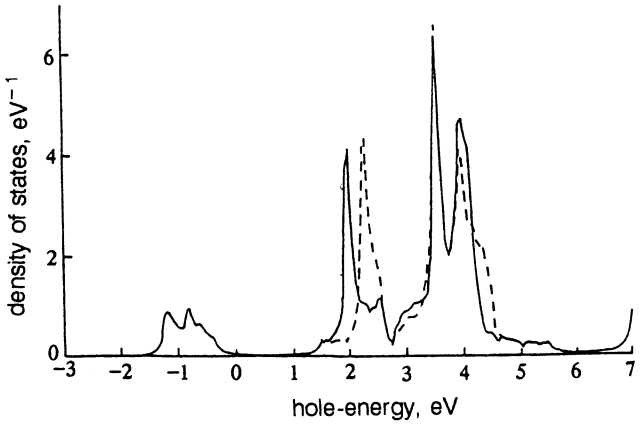

FIG. 5. Density of hole states for different ground states of a cluster with two holes: the dashed curve corresponds to a Zhang–Rice singlet, and the solid curve to a triplet.

ing to Pickett,[3] the t_{2g}-states of copper lie 4 eV below the top of the valence band, and in Fig. 2 they must appear in the dip at $E=5$–6 eV.

Figure 3 depicts the density of states as a function of the damping parameter ε. The reader can see that an increase in resolution results in a Van Hove singularity at the center of the conduction band. Near the top of the valence band the density of states remains practically unchanged.

The band structure of quasiparticles calculated in Refs. 7 and 10 and the quasiparticle density of states are compared in Fig. 4 (in the electron representation). The reader can see that not all quasiparticle bands result in peaks in the density of states. For some quasiparticles $F(m)\neq 0$ and the Green functions (5) are finite, with the result that there is a contribution to the solutions of the dispersion equation, but because the matrix elements $\gamma_\lambda(m)$ in (17) are equal to zero there is no contribution to the density of states. Near the top of the valence band the main contribution is provided by the p-d-hybridized bands, in which the p_0-states have the greatest weight (up to 85%). Near the bottom of the conduction band there are bands of the same symmetry but with $d_{x^2-y^2}$-states providing the decisive contribution.

Note that with our choice of the Hamiltonian parameters (18) the ground two-hole state is the spin triplet Ω_3, in contrast to the widely accepted notion that it is the Zhang–Rice singlet.[11] Since the energy difference $\Omega_3-\Omega_2$ is small, crossover may occur at fairly small variations of the parameters,[12] for instance, t_{pp}. Figure 5 shows two variants of the density of states, with the singlet and triplet ground states of a "hole on copper"+hole on oxygen" pair. An arm in the 1.4 eV $<E<$ 2.2 eV interval, a feature characteristic of the Zhang–Rice singlet, should appear in photoelectron emission spectra. There are several arguments in favor of the triplet state,[10] for instance, the nature of the dispersion law in the vicinity of the Γ-point: a minimum (in the electron representation) for the triplet and a maximum for the singlet. Experiments in photoelectron emission with angular resolution usually exhibit a minimum (see Pickett's review[3] and Ref. 5).

6. VARIATION OF THE DENSITY OF STATES UNDER HOLE DOPING

Under doping the number n of holes per cluster is $1+X$. Solutions to the self-consistency equation for the occupation numbers have the form

$$\langle X^{1,\sigma;1,\sigma}\rangle=\frac{1-x}{2}.$$

For the lower state with $n=2$, the singlet,

$$\langle X^{2,0,0,0;2,0,0,0}\rangle=x,\quad \langle X^{2,0,1,M;2,0,1,M}\rangle=0.$$

For the lower triplet,

$$\langle X^{2,0,0,0;2,0,0,0}\rangle=0,\quad \langle X^{2,0,1,M;2,0,1,M}\rangle=\tfrac{1}{3}x.$$

Thus, the single-particle ground states of the CuO_4 cluster are filled with a probability $1-x$ and the two-particle states are filled with the probability x. The result are new Fermi quasiparticles with $D(m)\sim x$.

Figure 6 depicts the density of hole states calculated with parameters (18) but with a new value of V_{pd} equal to 1 eV. This variation was done for a more distinct separation of the new states from the bottom of the conduction band. Although no common impurity effects such as potential fluctuations or fluctuations of the parameters of Hamiltonian (1) were introduced and the only variable quantity was the carrier concentration, the states that

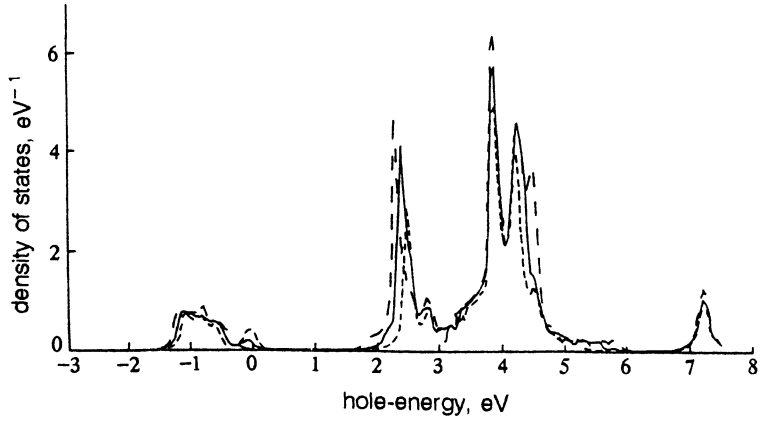

FIG. 6. Variation of the density of states under hole doping. The long-dash curve corresponds to concentration $X=0$, the solid curve to 0.15, and short-dash curve to 0.30.

formed inside the gap were found to behave like impurity states: the density of states on them was proportional to concentration X.

According to Ref. 14, new states appear upon doping for all values of the Hamiltonian parameters, but very rarely find themselves inside the dielectric gap. An important factor in this case is the copper-oxygen Coulomb interaction. As V_{pd} increases, the localized level moves from the edge of the gap to the center.

Thus, in the multielectron theory the picture of a rigid band is not true. The fact that states appear inside the gap following doping in copper oxides has been firmly established from spectroscopic data.[15] The appearance of states in the gap upon doping was predicted earlier in cluster calculations in the process of exact diagonalization of model Hamiltonians of type (1) or its simpler variants.[16,19]

The fact that under hole doping an impurity level appears close to the bottom of the conduction band rather than close to the top of the valence band has no special meaning (although it agrees with the data of Ref. 4). The point is that in a more realistic approach one must allow for impurity effects, the simplest of which is the variation of the parameters of Hamiltonian (1) in the neighborhood of a carrier. Indeed the ion radius of O^- is smaller than that of O^{2-}, as noted by many researchers.[20,21] For instance, according to Kulik,[21] in the octahedral surroundings $R(O^-)=1.36$ Å. Hence, when the carrier is on oxygen, the most obvious variation of the parameter is to lower T_{pd}. In addition, the hole levels ε_p and ε_d shift in the crystalline field. Estimates in the point-charge model point to a decrease in the parameter $\delta=\varepsilon_p-\varepsilon_d$ by approximately one electron volt. The role of variations of T_{pd} and δ has been examined in Ref. 22 by the method of exact diagonalization of the Hamiltonian (1) for the CuO_4 cluster. It was found that, owing to variations in the parameters in the vicinity of a carrier, levels appear near the top of the valence band in addition to those considered above. A similar calculation for an infinite crystal lies outside the scope of the present work.

7. CONCLUSION

The suggested method of calculating the density of single-particle states, which allows for multielectron effects, makes it possible to calculate the density of states of various copper oxides. The set of parameters (18) considered corresponds to La_2CuO_4; for Nd_2CuO_4; the basic difference (the absence of ohmic oxygen) is reduced to the decrease in the value of $\delta=\varepsilon_p-\varepsilon_d$ (see Refs. 7 and 23). Thus, varying the parameters of Hamiltonian (1) makes it possible to model various copper oxides.

For hole doping, the present calculation for an infinite crystal supports the earlier conclusion obtained from cluster calculations[16–19] that new states appear in the gap. As noted by Eskes and Sawatzky,[24] neither the accuracy of calculating small clusters nor the Anderson impurity model is sufficient for discussing the details of the structure of the top of the valence band, details that are necessary for a more qualitative comparison with the experimental data. Our calculation allows for the details of the band structure of an infinite crystal combined with an exact cluster diagonalization.

The work was sponsored by the Krasnoyarsk Science Fund under Grant Number IF0014.

APPENDIX

All components M_{ij} with an even sum of indices, $i+j$, are zero, and the nonzero components are

$$M_{1,2}=A_1F^{11}_{12}+A_2F^{11}_{13},\quad M_{1,4}=A_3F^{11}_{11}+B_1F^{11}_{12}+B_3F^{11}_{13},\quad M_{1,6}=A_4F^{11}_{11}+B_2F^{11}_{12},\quad M_{1,8}=B_4F^{11}_{14}+B_7F^{11}_{15},$$

$$M_{1,10}=B_5F^{11}_{14}+B_6F^{11}_{15},\quad M_{2,1}=A^*_3F^{22}_{12}+A^*_4F^{22}_{13},\quad M_{2,3}=A^*_1F^{22}_{11}+B^*_1F^{22}_{12}+B^*_2F^{22}_{13},\quad M_{2,5}=A^*_2F^{22}_{11}+B^*_3F^{22}_{11},$$

$$M_{2,7}=B^*_4F^{22}_{14}+B^*_5F^{22}_{15},\quad M_{2,9}=B^*_6F^{22}_{15}+B^*_7F^{22}_{14},\quad M_{3,2}=A_1F^{11}_{22}+A_2F^{11}_{23},\quad M_{3,4}=A_3F^{11}_{12}+B_1F^{11}_{22}+B_3F^{11}_{23},$$

$$M_{3,6}=A_4F^{11}_{12}+B_2F^{11}_{22},\quad M_{3,8}=B_4F^{11}_{24}+B_7F^{11}_{25},\quad M_{3,10}=B_5F^{11}_{24}+B_6F^{11}_{25},\quad M_{4,1}=A^*_3F^{22}_{22}+A^*_4F^{22}_{23},$$

$$M_{4,3}=A^*_1F^{22}_{12}+B^*_1F^{22}_{22}+B^*_2F^{22}_{23},\quad M_{4,5}=A^*_2F^{22}_{12}+B^*_3F^{2}_{22},\quad M_{4,7}=B^*_4F^{22}_{24}+B^*_5F^{22}_{25},\quad M_{4,9}=B^*_6F^{22}_{25}+B^*_7F^{22}_{24},$$

$$M_{5,2}=A_1F^{11}_{23}+A_2F^{11}_{33},\quad M_{5,4}=A_3F^{11}_{13}+B_1F^{11}_{23}+B_2F^{11}_{33},\quad M_{5,6}=A_4F^{11}_{13}+B_2F^{11}_{23},\quad M_{5,8}=B_4F^{11}_{34}+B_7F^{11}_{35},$$

$$M_{5,10}=B_5F^{11}_{34}+B_6F^{11}_{35},\quad M_{6,1}=A^*_3F^{22}_{23}+A^*_4F^{22}_{33},\quad M_{6,3}=A^*_1F^{22}_{13}+B^*_1F^{22}_{23}+B^*_2F^{22}_{33},\quad M_{6,5}=A^*_2F^{22}_{13}+B_3F^{22}_{23},$$

$$M_{6,7}=B^*_4F^{22}_{34}+B^*_5F^{22}_{35},\quad M_{6,9}=B^*_6F^{22}_{35}+B^*_7F^{22}_{34},\quad M_{7,2}=A_1F^{11}_{24}+A_2F^{11}_{34},\quad M_{7,4}=A_3F^{11}_{14}+B_1F^{11}_{24}+B_3F^{11}_{34},$$

$$M_{7,6}=A_4F^{11}_{14}+B_2F^{11}_{24},\quad M_{7,8}=B_4F^{11}_{44}+B_7F^{11}_{45},\quad M_{7,10}=B_5F^{11}_{44}+B_6F^{11}_{45},\quad M_{8,1}=A^*_3F^{22}_{24}+A^*_4F^{22}_{34},$$

$$M_{8,3}=A^*_1F^{22}_{14}+B^*_1F^{22}_{24}+B^*_2F^{22}_{34},\quad M_{8,5}=A^*_2F^{22}_{14}+B^*_3F^{22}_{24},\quad M_{8,7}=B^*_4F^{22}_{44}+B^*_5F^{22}_{45},\quad M_{8,9}=B^*_6F^{22}_{45}+B^*_7F^{22}_{44},$$

$$M_{9,2}=A_1F^{11}_{25}+B_2F^{11}_{35},\quad M_{9,4}=A_3F^{11}_{15}+B_1F^{11}_{25}+B_3F^{11}_{35},\quad M_{9,6}=A_4F^{11}_{15}+B_2F^{11}_{25},\quad M_{9,8}=B_4F^{11}_{45}+B_7F^{11}_{55},$$

$$M_{9,10}=B_5F^{11}_{45}+B_6F^{11}_{55},\quad M_{10,1}=A^*_3F^{22}_{25}+A^*_4F^{22}_{35},\quad M_{10,3}=A^*_1F^{22}_{15}+B^*_1F^{22}_{25}+B^*_2F^{22}_{35},\quad M_{10,5}=A^*_2F^{22}_{15}+B^*_3F^{22}_{25},$$

$$M_{1,2}=A_1F^{11}_{12}+A_2F^{11}_{13},\quad M_{10,7}=B^*_4F^{22}_{45}+B^*_5F^{22}_{55},\quad M_{10,9}=A^*_6F^{22}_{55}+B^*_7F^{22}_{45}.$$

[1] J. Zaanen, G. A. Sawatzky, and G. W. Allen, Phys. Rev. Lett. **55**, 410 (1985).
[2] N. F. Mott, *Metal-Insulator Transitions*, 2nd ed., Taylor & Francis, London (1990).
[3] W. E. Pickett, Rev. Mod. Phys. **61**, 433 (1989).
[4] A. Fujimori and H. Namatame, Physica C **185–189**, 51 (1991).
[5] S. G. Ovchinnikov and I. S. Sandalov, Physica C **161**, 607 (1989).
[6] S. G. Ovchinnikov and O. G. Petrakovskiĭ, Sverkhprovodimost': Fiz. Khim. Tekhnol. **3**, 2492 (1990).
[7] S. G. Ovchinnikov, Zh. Eksp. Teor. Fiz. **102**, 127 (1992) [Sov. Phys. JETP **75**, 67 (1992)].
[8] V. V. Val'kov, T. A. Val'kova, and S. G. Ovchinnikov, Zh. Eksp. Teor. Fiz. **88**, 550 (1985) [Sov. Phys. JETP **62**, 313 (1985)].
[9] R. O. Zaĭtsev, Zh. Eksp. Teor. Fiz. **68**, 207 (1975) [Sov. Phys. JETP **41**, 100 (1975)].
[10] S. G. Ovchinnikov and O. G. Petrakovsky, J. Superconductivity **4**, 437 (1991).
[11] F. C. Zhang and T. M. Rice, Phys. Rev. B **37**, 3559 (1988).
[12] S. G. Ovchinnikov, Mod. Phys. Lett. **5**, 531 (1991).
[13] W. Stephan and P. Horsch, in *Dynamics of Magnetic Fluctuations in High-Temperature Superconductors*, edited by G. Reiter *et al.*, Plenum Press, New York (1991).
[14] S. G. Ovchinnikov, Zh. Eksp. Teor. Fiz. **102**, 534 (1992) [Sov. Phys. JETP **75**, 283 (1992)].
[15] T. Kusunoki, T. Kahashi, S. Sato, H. Katayama-Yoshida, K. Kamiya, and H. Inokuchi, Physica C **185–189**, 1045 (1991).
[16] P. Horsch, W. H. Stephan, K. v. Szczepanski, M. Ziegler, and W. von der Linden, Physica C **162–164**, 783 (1989).
[17] D. J. Scalapino, Physica C **185–189**, 104 (1991).
[18] E. Dagotto, Physica C **185–189**, 1629 (1991).
[19] T. Tohyama and S. Maekawa, Physica C **191**, 193 (1992).
[20] G. G. Khaliullin, JETP Lett. **49**, [*sic*] (1989).
[21] I. O. Kulik, Sverkhprovodimost': Fiz. Khim. Tekhnol. **2**, 175 (1989).
[22] S. G. Ovchinnikov, Zh. Eksp. Teor. Fiz. **103**, 1404 (1993) [Sov. Phys. JETP **76**, 687 (1993)].
[23] Y. Ohta, T. Tohyama, and S. Maekawa, Phys. Rev. Lett. **66**, 1228 (1991).
[24] H. Eskes and G. A. Sawatzky, Phys. Rev. B **44**, 9656 (1991).

Translated by Eugene Yankovsky

This article was translated in Russia and is reproduced here the way it was submitted by the translator, except for stylistic changes by the Translation Editor.